PCCP

Accepted Manuscript

ROYAL SOCIETY OF CHEMISTRY

www.rsc.org/pccp

Cite this: DOI: 10.1039/c0xx00000x

www.rsc.org/xxxxxx

ARTICLE TYPE

Stability domain of the selenide kesterite photovoltaic materials and NMR investigation of Cu/Zn disorder in $Cu_2ZnSnSe_4$ (CZTSe).

Léo Choubrac,[a] Alain Lafond,*[a] Michaël Paris,[a] Catherine Guillot-Deudon,[a] and Stephane Jobic [a]

Received (in XXX, XXX) Xth XXXXXXXXX 20XX, Accepted Xth XXXXXXXXX 20XX

DOI: 10.1039/b000000x

Bulk compounds, prepared by ceramic route, related to $Cu_2ZnSnSe_4$ (CZTSe), a material considered for use in photovoltaic devices, were investigated using NMR spectroscopy, Electron-Probe Micro Analyses and X-ray diffraction. These materials adopt the kesterite structure regardless the Cu and Zn contents. It is also shown that the stability domain of the copper-poor quaternary phases is wider for selenide derivatives than for sulphides. Finally, the Cu/Zn disorder level in CZTSe is found to be higher when the samples are quenched which reminds the behaviour of the sulphide parent compounds CZTS.

Compared to silicon-based technologies thin film-based solar cells are expected to save materials and to have a shorter energy pay-back time. Copper zinc tin chalcogenide materials (Cu_2ZnSnQ_4, Q = S or/and Se, noted CZTS, CZTSe or CZTSSe) are extensively investigated as potential photovoltaic absorbers for such thin-film solar cells[1–3]. These materials contain non-toxic and earth abundant elements and reach so far energy conversion efficiencies up to 12.6%[4]. The best performances are always obtained for Cu-poor compounds[5] containing both sulfur and selenium[6]. Secondary phases should be avoided in high-performance cells.. Thus, it is essential to understand the extent of the CZTQ phase stability domain in the Cu_2Q-ZnQ-SnQ_2 ternary diagram in detail.

Such investigation has already been carried out on pure sulphide compounds through a solid state chemistry approach built upon X-ray diffraction and NMR spectroscopy[7,8]. So far, two main substitution processes have been considered to account for the charge balance in Cu-poor CZTS materials. Namely, the A-type substitution $2Cu \rightarrow V_{Cu} + Zn_{Cu}$ (with a formulation of $Cu_{2-2a}Zn_{1+a}SnS_4$) and the B-type substitution $2Cu + Sn \rightarrow 2Zn_{Cu} + Zn_{Sn}$ ($Cu_{2-2b}Zn_{1+3b}Sn_{1-b}S_4$). The main result of this previous study was that the lowest copper-content in Cu-poor CZTS compound ($Cu_{1.705}Zn_{1.185}Sn_{0.98}S_4$) is achieved when A and B-type defects (AB-substitution) coexist[9].

The crystal structure of CZTS compounds has been intensively studied because of its potential impact on the electronic properties of these semiconductors. On the other hand the crystal structure of the selenide series is still open.

In this communication, we present both NMR investigation of the local crystal structure and a detailed study of the CZTSe phase stability boundaries under the copper-poor, zinc-rich compositions. Additionally, these compounds have been investigated using both powder and single crystal X-ray diffraction. These results are compared to those reported for the sulphide derivatives.

Experimental

The studied samples (see Table 1) have been synthesized via the ceramic method from elemental precursors heated at 750°C in evacuated, sealed, fused silica tubes (see ESI). In order to investigate the Cu/Zn disorder in CZTSe compounds, some samples underwent specific thermal treatments after synthesis. Hence, two new samples have been obtained from sample A2, $A2_Q$ (quenched) and $A2_S$ (slow cooled) after annealing at 350°C for 2 days.

The sample homogeneity was checked by powder X-ray diffraction and the unit cell parameters of the compounds were obtained by the refinement of the corresponding patterns by the Le Bail method (full pattern matching mode) with the use of the Jana2006 program[10]. The chemical compositions of the studied samples were accurately determined by Electron-Probe Micro Analyses (EPMA) on polished sections.

For the structure analysis, a single crystal suitable for X-ray diffraction was picked up from the sample S3 which is not strictly at stoichiometry However, during the structure refinement the choosen single crystal appeared to be very close to the $Cu_2ZnSnSe_4$ composition.

In a previous study solid state NMR spectroscopy was shown to be a powerful tool to investigate the local structure in CZTS materials[11]. So, ^{65}Cu and ^{119}Sn NMR investigations were performed on the studied selenide CZTSe samples. Additionally, the Raman spectra were recorded at 514.5 nm excitation wavelength in back scattering configuration on a high resolution spectrometer. Attention was paid to the power density of the incident laser which was adjusted to avoid any modification on the recorded spectra.

Details about the experimental conditions for all the used characterization techniques are given in ESI.

Results and discussion

Crystal structure

After much controversy, it is now well established that CZTS materials crystallize with the kesterite (KS) structure, in its

ordered or disordered forms depending on prior thermal treatments[7,12]. In the case of the selenide derivative, $Cu_2ZnSnSe_4$, the first crystal investigations ascribed the stannite structure[13,14]. Formally, the main difference between these two polymorphs, both deriving from the ZnS-sphalerite structure type, is related to the occupation of the 2a Wyckoff position ((000) coordinates) by Cu in kesterite and Zn in stannite. Consequently, there are two distinct crystallographic sites for copper in kesterite (2*a* and 2*c*) while there is only one in stannite (4*d*). Recently, Nateprov et al.[15] concluded that the actual crystal structure of $Cu_2ZnSnSe_4$ is kesterite. Although the conclusion turn out to be correct, this study appears to suffer from a lack of precision (see ESI) so we decided to reinvestigate the crystal structure of the stoichiometric $Cu_2ZnSnSe_4$. Even though, it is difficult to distinguish between Cu and Zn using conventional X-ray diffraction, our data shows that the kesterite structure (more precisely, the disordered-kesterite, see the *Cu/Zn disorder* section) is the most representative model. Our measured residual factors R(obs)/wR(obs) are 3.06/10.97 and 2.75/9.94 for stannite and kesterite respectively (411 observed unique reflections and 14 refined parameters in the *I*-42*m* space group). Details about this structure investigation are given in ESI. The corresponding CIF file has been deposited with the Cambridge Crystallographic Data Centre (CCDC reference number: CCDC 1054041).

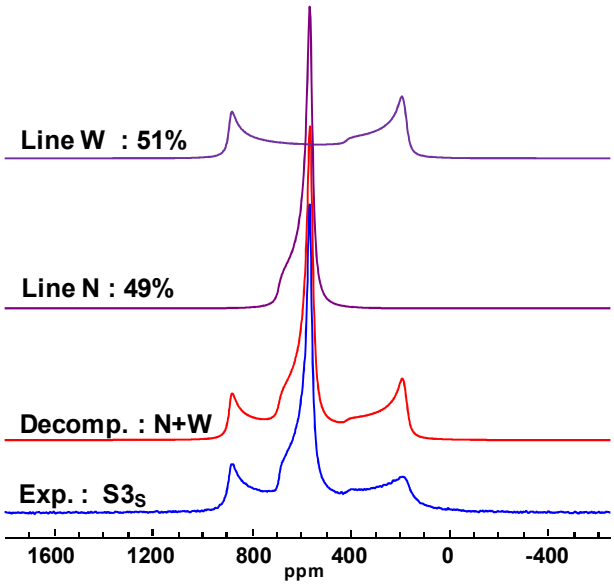

Fig. 1: ^{65}Cu static NMR (blue) with spectral decomposition (red) for $Cu_2ZnSnSe_4$ compound in 2 individual lines (purple). The NMR parameters are C_Q=5.5 MHz, η_Q=0, δ_{iso}=600 ppm δ_{aniso}=-183 ppm η_δ=0 and β=2° for line W and C_Q=1.5 MHz, η_Q=0, δ_{iso}=596 ppm δ_{aniso}=95ppm η_δ=0 and β=0° for line N. (Details in ESI).

The correctness of the proposed structural model for $Cu_2ZnSnSe_4$ is strongly supported by the ^{65}Cu NMR investigation. Indeed, the ^{65}Cu static NMR spectrum of the sample (Fig. 1) can be efficiently fitted by a wide (W, C_Q = 5.5 MHz) and a narrow (N, C_Q = 1.5 MHz) lines with lineshapes reflecting both the chemical shift and the quadrupolar interactions. All the experimental values of the NMR parameters are gathered in Fig. 1. From the single crystal structure refinement presented above, the 2*a* site appears much more distorted than the 2*c* site, leading to a larger Electric Field Gradient (EFG) at 2*a* site and therefore, to a larger C_Q. Thus, the lines W and N are assigned to the 2*a* and the 2*c* sites, respectively. This attribution is supported by the values of the quadrupolar coupling, C_Q=5.8 MHz / η_Q=0 for the 2*a* site and C_Q=1.8 MHz / η_Q=0 for the 2*c* site, obtained from DFT calculations carried out on a hypothetical ordered kesterite structure[16]. In addition, the two spectral NMR lines have the same intensity which agrees perfectly with the 2-fold multiplicity of the 2 copper sites within the kesterite structure and definitively rebut the stannite structure.

A similar ^{65}Cu static NMR investigation has been performed for a Cu-poor Zn-rich selenide compound (sample A2) showing also a 2-component spectrum (see Figure SI1 in ESI). This result clearly suggests that the whole CZTSe compounds adopt the kesterite crystal structure, Cu at 2 distinguishable sites, regardless of their actual compositions.

Quaternary phase stability domain

Dudchak et al.[17] have deeply investigated the phase equilibria in the Cu_2Se-ZnSe-$SnSe_2$ system but they do not focus specifically on the $Cu_2ZnSnSe_4$ compound.

A large set of samples was prepared and most of them did not appear to be homogeneous. The analyses were performed only on the grains corresponding to quaternary phases. Because the target compositions were far from the stoichiometry of $Cu_2ZnSnSe_4$, the phase stability boundaries of the quaternary CZTSe are expected to be reached. The target and average compositions of these samples determined from microprobe analyses are gathered in Table 1 and represented in the pseudo-ternary Cu_2Se/ZnSe/$SnSe_2$ diagram in Fig. 2.

Table 1: Targeted composition of the studied samples and the corresponding average compositions from microprobe analyses.

Label	Targeted composition	Average composition
S1	$Cu_{2.00}Zn_{1.00}Sn_{1.00}Se_{4.00}$	$Cu_{1.999}Zn_{1.010}Sn_{0.995}Se_4$
S2	$Cu_{2.00}Zn_{1.00}Sn_{1.00}Se_{4.00}$	$Cu_{1.936}Zn_{0.964}Sn_{1.039}Se_4$
S3	$Cu_{2.00}Zn_{1.00}Sn_{1.00}Se_{4.00}$	$Cu_{1.911}Zn_{1.011}Sn_{1.036}Se_4$
A1	$Cu_{1.80}Zn_{1.10}Sn_{1.00}Se_{4.00}$	$Cu_{1.828}Zn_{1.128}Sn_{0.978}Se_4$
A2	$Cu_{1.70}Zn_{1.15}Sn_{1.00}Se_{4.00}$	$Cu_{1.751}Zn_{1.196}Sn_{0.957}Se_4$
A3	$Cu_{1.60}Zn_{1.20}Sn_{1.00}Se_{4.00}$	$Cu_{1.640}Zn_{1.290}Sn_{0.945}Se_4$(*)
A4	$Cu_{1.40}Zn_{1.30}Sn_{1.00}Se_{4.00}$	$Cu_{1.693}Zn_{1.239}Sn_{0.951}Se_4$
B1	$Cu_{1.90}Zn_{1.15}Sn_{0.95}Se_{4.00}$	$Cu_{1.925}Zn_{1.061}Sn_{0.966}Se_4$
AB1	$Cu_{1.71}Zn_{1.28}Sn_{0.933}Se_{4.00}$	$Cu_{1.984}Zn_{1.065}Sn_{0.987}Se_4$ (AB1-1)
AB1	$Cu_{1.71}Zn_{1.28}Sn_{0.933}Se_{4.00}$	$Cu_{1.936}Zn_{1.147}Sn_{0.972}Se_4$ (AB1-2)
AE1	$Cu_{1.70}Zn_{1.05}Sn_{1.05}Se_{4.00}$	$Cu_{1.765}Zn_{1.105}Sn_{0.987}Se_4$
AE2	$Cu_{1.50}Zn_{1.12}Sn_{1.065}Se_{4.00}$	$Cu_{1.589}Zn_{1.168}Sn_{1.009}Se_4$

* A3 sample appeared to be highly inhomogeneous, the given value corresponds to one spot analysis only. It corresponds to the more Cu-poor Zn-rich CZTSe prepared compound.

The above presented substitution processes (A and B) are indicated by dashed lines in Fig. 2.

Moreover, we propose to introduce here, based on experimental investigations, a new substitution type named E-type that differs from A, B, C and D types discussed in a previous paper[9]. Namely, this new substitution process would consist of the replacement of two Cu and one Zn cations by one Sn cation with the appearance of two copper vacancies ($2Cu + Zn \rightarrow 2V_{Cu} + Sn_{Zn}$) leading to the overall $Cu_{2-2e}Zn_{1-e}Sn_{1+e}Se_4$ formulation (vertical straight line in the ternary diagram). Then, a composition above the horizontal A line in Fig. 2 (Sn-rich side) can be viewed as a combination of the A and E substitutions leading to a general $Cu_{2-2a-2e}Zn_{1+a-e}Sn_{1+e}Se_4$ formulation.

The limits of the studied stability diagram correspond to the following compositions $Cu_{1.59}Zn_{1.17}Sn_{1.01}Se_4$ (sample AE2, A+E-type), $Cu_{1.94}Zn_{1.15}Sn_{0.97}Se_4$ (sample AB1-2, B-type) and $Cu_{1.64}Zn_{1.29}Sn_{0.945}Se_4$ (sample A3, A+B-type).

Clearly, the stability domain of the CZTSe phase extends to the Sn-rich region (light grey in Fig. 2), a region rarely discussed and that would probably deserve further investigations not reported here.

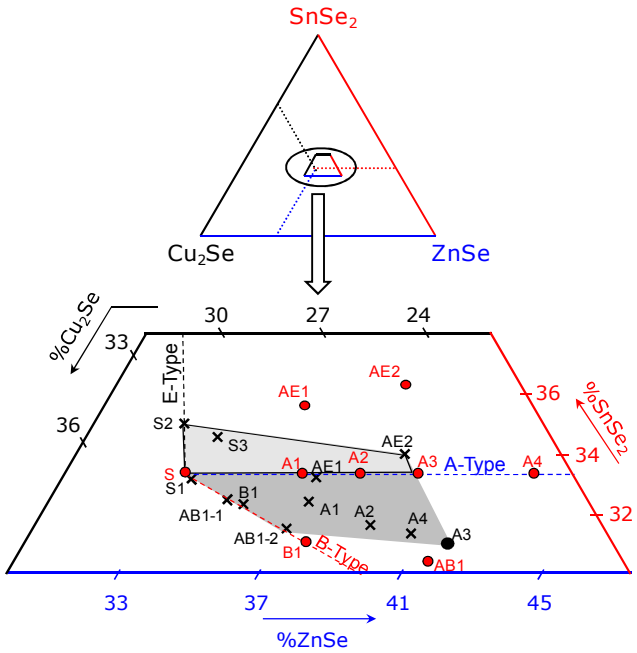

Fig. 2: Stability domain of the copper-poor quaternary kesterite phases in the Cu_2Se-ZnSe-$SnSe_2$ diagram. The full red circles indicate the targeted compositions and the black crosses the average compositions of the corresponding quaternary phases. The targeted composition for S1, S2 and S3 is the stoichiometric Cu_2ZnSnS_4 (S full red circle).

Cu/Zn disorder

Let us now present the study of the Cu/Zn disorder in CZTSe by local probe measurements. In the kesterite structure, the two cationic site at z=1/4 and z=3/4, namely the 2*c* and 2*d* Wyckoff positions, are crystallographically very similar. In the fully ordered kesterite structure Cu and Zn atoms are located on 2*c* and 2*d* sites respectively. This distribution can be perturbed according to the thermal history of the sample. If the cationic distribution is fully random (site occupancies of 50% for Cu and Zn on both sites) the structure becomes the full disordered kesterite (dis-KS) with a higher symmetry[18] (i.e. *I*-42*m* instead of *I*-4, see Figure SI2). The single crystal structure of the stoichiometric CZTSe (*vide supra*) has been refined with the dis-KS model.

The influence of the cooling procedure at the end of the sample preparation on the Cu/Zn disorder has been investigated with the help of ^{119}Sn NMR spectroscopy as well as Raman spectroscopy. This investigation was restricted to the quenched and slow cooled samples prepared with an actual $Cu_{1.751}Zn_{1.196}Sn_{0.957}Se_4$ composition (samples $A2_Q$ and $A2_S$). At very first sight, the impact of the cooling procedure was directly visible on the powder diffraction pattern for the c/a ratios are 1.9938(1) and 1.99120(6) for $A2_Q$ and $A2_S$, respectively. This trend, a higher c/a ratio when the sample is quenched, was already noticed for the CZTS materials[8].

Fig. 3 gives the ^{119}Sn MAS NMR spectra of samples $A2_Q$ and $A2_S$. In agreement with results previously obtained on sulphide compounds, the spectrum $A2_S$ consists of two resonances. The main resonance at -592 ppm is associated with the ordered kesterite structure of $Cu_2ZnSnSe_4$ whereas the second at -544 ppm is associated with Sn atoms experiencing Cu vacancies in their second coordination shell. For the quenched sample ($A2_Q$) both the ^{119}Sn (Fig. 3) and ^{65}Cu (Fig. SI1 in ESI) NMR spectra are broadened. The latter becomes featureless even if the two Cu resonances of the KS structure are still distinguishable. In addition, an asymmetric broadening, as well as a slight right shift (~-12 ppm), of the two ^{119}Sn resonances are observed. This reflects an isotropic chemical shift distribution coming from a distribution of ^{119}Sn environments due to the existence of geometric (angles and distances) and chemical disorders.

These observations can be correlated to the high level of Cu/Zn disorder, in the quenched sample, as it was proposed for the sulphide parent compounds[11].

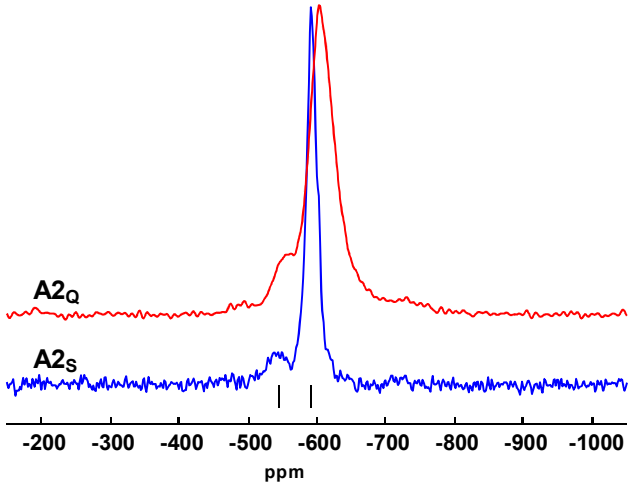

Fig. 3: ^{119}Sn MAS NMR spectra for A-type sample $A2_S$ and $A2_Q$ ($Cu_{1.751}Zn_{1.196}Sn_{0.957}S_4$). Ticks indicate the line positions for $A2_S$, -592 and -544 ppm.

Finally, the Cu/Zn disorder has been tracked through Raman spectroscopy on the same $A2_Q$ and $A2_S$ samples. The corresponding spectra are given in Figure SI3, in ESI. In agreement with the literature[19–21], the main peaks of the slow cooled sample are found to be at 168, 172 and 195 cm^{-1}. There is a slight peak shift toward low frequencies for the quenched sample but the main effect going from slow cooled to quenched samples concerns the peak broadening. These observations perfectly agree with a recent study on the Cu/Zn disorder on CZTSe thin films which pointed out an order-disorder transition temperature of about 200°C[22].

Conclusion: comparison with sulphides

The above presented results are reminiscent of those for sulphide CZTS compounds[8]. In particular (i) the kesterite structure is the preferred structure for CZTS and CZTSe compounds, (ii) the ^{65}Cu NMR is not very sensitive to the actual composition, (iii) ^{119}Sn NMR can be used to monitor the presence of copper vacancies, (iv) ^{65}Cu and ^{119}Sn NMR as well as the Raman spectroscopy are highly dependent on the Cu/Zn disorder level.

The main difference between ^{119}Sn spectra for sulphides and selenides is the overall line shift of about 470 ppm due to the replacement of S by Se (See Fig. SI4).

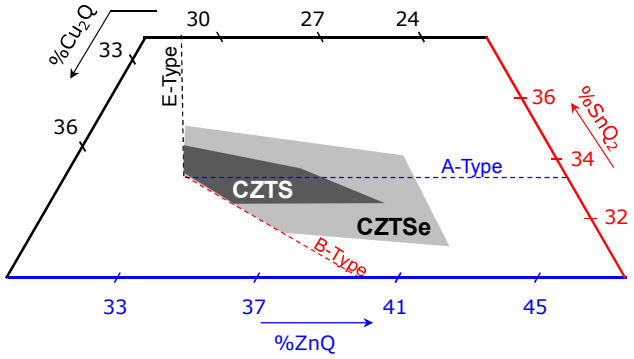

Fig. 4: Comparison of the quaternary phase stability domains for CZTS and CZTSe.

In our previous NMR investigations on sulphide compounds, we introduced the actual number (N) of Sn atoms affected per Cu vacancy[8]; the Cu-vacancy content being deduced from the measured composition. From the determination of a value of N close to 2 (rather than 4 as expected for isolated A-type complexes), we concluded to the propensity of A-type complexes to segregate in CZTS. We applied the same approach for the samples $A2_S$ and $A2_Q$ and found N values close to 1 (N equals to ~1 and ~0.8 for $A2_S$ and $A2_Q$, respectively). Such a value is very unlikely because it would correspond to a severe aggregation of the A-type complexes which could lead to strong local distortions of the crystallographic structure. In our opinion, these low values rather suggest that our previous assumption that V_{Cu} located only at the 2*a* site, is not fulfilled anymore in selenide compounds. Further work, coupling NMR and X-ray investigations, is needed to address this point.

Differences in cation compensation between sulphides and selenides might be related to the difference in the extent of their phase domain stability. Indeed, as shown in Fig. 4, larger shifts from the nominal stoichiometry Cu_2ZnSnQ_4 (Q=S or Se) are observed for selenides. Thus one can conclude that selenides are much more flexible to be more copper-poor zinc rich than sulphides. This result could be related to the enhancement of photovoltaic performances when S is partially replaced by Se in CZTSSe.

Acknowledgements

The technical assistance of J. Langlade (IFREMER-Brest-France) for microprobe analyses and of J. Y. Mevellec (IMN) for Raman spectroscopy are acknowledged. The authors also acknowledge the financial support of the French ANR under Grant NovACEZ (ANR-10- HABISOL-008).

Notes and references

[a] *Institut des Matériaux Jean Rouxel (IMN), Université de Nantes, CNRS. 2, rue de la Houssinière, BP 32229, 44322 Nantes Cedex 03, France . Tel: +33 240 373 939*
**E-mail: alain.lafond@cnrs-imn.fr*
Present adress of Léo Choubrac: Laboratory for Photovoltaics, 162 A, avenue de la Faïencerie L-1511 Luxembourg (leo.choubrac@uni.lu)

† Electronic Supplementary Information (ESI) available: details for the preparation and the standard characterization of the samples, Crystallographic data for $Cu_2ZnSnSe_4$, the coordinates of the compositions of the studied samples in the Cu2Se/ZnSe/SnSe2 ternary diagram and additional NMR and Raman spectra.

1. H. Katagiri, N. Ishigaki, T. Ishida and K. Saito, *Jpn J Appl Phys Part 1*, 2001, **40**, 500–504.
2. S. Abermann, *Sol. Energy*, 2013, **94**, 37–70.
3. S. Siebentritt and S. Schorr, *Prog. Photovolt. Res. Appl.*, 2012, **20**, 512–519.
4. W. Wang, M. T. Winkler, O. Gunawan, T. Gokmen, T. K. Todorov, Y. Zhu and D. B. Mitzi, *Adv. Energy Mater.*, 2014, **4**, 1301465.
5. H. Katagiri, K. Jimbo, M. Tahara, H. Araki and K. Oishi, in *Materials Research Society Symposium Proceedings*, 2009, p. 1165.
6. K. Timmo, M. Altosaar, J. Raudoja, K. Muska, M. Pilvet, M. Kauk, T. Varema, M. Danilson, O. Volobujeva and E. Mellikov, *Sol. Energy Mater. Sol. Cells*, 2010, **94**, 1889–1892.
7. L. Choubrac, A. Lafond, C. Guillot-Deudon, Y. Moëlo and S. Jobic, *Inorg Chem*, 2012, **51**, 3346–3348.
8. M. Paris, L. Choubrac, A. Lafond, C. Guillot-Deudon and S. Jobic, *Inorg. Chem.*, 2014, **53**, 8646–8653.
9. A. Lafond, L. Choubrac, C. Guillot-Deudon, P. Deniard and S. Jobic, *Z Anorg Allg Chem*, 2012, 2571–2577.
10. V. Petříček, M. Dušek and L. Palatinus, *Z. Für Krist. - Cryst. Mater.*, 2014, **229**, 345–352.
11. L. Choubrac, M. Paris, A. Lafond, C. Guillot-Deudon, X. Rocquefelte and S. Jobic, *Phys. Chem. Chem. Phys.*, 2013, **15**, 10722.
12. S. Schorr, *Sol. Energy Mater. Sol. Cells*, 2011.
13. L. Guen and W. S. Glaunsinger, *J. Solid State Chem.*, 1980, **35**, 10–21.
14. I. D. Olekseyuk, L. D. Gulay, I. V. Dydchak, L. V. Piskach, O. V. Parasyuk and O. V. Marchuk, *J. Alloys Compd.*, 2002, **340**, 141–145.
15. A. Nateprov, V. C. Kravtsov, G. Gurieva and S. Schorr, *Surf. Eng. Appl. Electrochem.*, 2013, **49**, 423–426.
16. L. Choubrac, PhD thesis, Université de Nantes, 2014.
17. I. V. Dudchak and L. V. Piskach, *J. Alloys Compd.*, 2003, **351**, 145–150.
18. A. Lafond, L. Choubrac, C. Guillot-Deudon, P. Fertey, M. Evain and S. Jobic, *Acta Crystallogr. Sect. B Struct. Sci. Cryst. Eng. Mater.*, 2014, **70**, 390–394.
19. M. Dimitrievska, H. Xie, A. Fairbrother, X. Fontané, G. Gurieva, E. Saucedo, A. Pérez-Rodríguez, S. Schorr and V. Izquierdo-Roca, *Appl. Phys. Lett.*, 2014, **105**, 031913.
20. M. Dimitrievska, G. Gurieva, H. Xie, A. Carrete, A. Cabot, E. Saucedo, A. Pérez-Rodríguez, S. Schorr and V. Izquierdo-Roca, *J. Alloys Compd.*, 2015, **628**, 464–470.
21. M. Grossberg, J. Krustok, K. Timmo and M. Altosaar, *Thin Solid Films*, 2009, **517**, 2489–2492.
22. G. Rey, A. Redinger, J. Sendler, T. P. Weiss, M. Thevenin, M. Guennou, B. E. Adib and S. Siebentritt, *Appl. Phys. Lett.*, 2014, **105**, 112106.